Few-Body Syst (2013) 54:647–656
DOI 10.1007/s00601-012-0468-1

**M. Viviani · L. Girlanda · A. Kievsky · L. E. Marcucci**

# Recent Progress in Ab-initio Four-Body Scattering Calculations

Received: 11 May 2012 / Accepted: 7 June 2012 / Published online: 6 July 2012


**Abstract** In the first part of the contribution, we discuss the results of a recent benchmark calculation of $n - {}^3\mathrm{H}$ and $p - {}^3\mathrm{He}$ phase-shifts below the trinucleon disintegration thresholds. Three different methods—Alt, Grassberger and Sandhas, Hyperspherical Harmonics, and Faddeev–Yakubovsky—have been used and their results are compared. For both $n - {}^3\mathrm{H}$ and $p - {}^3\mathrm{He}$ we observe a rather good agreement between the three different theoretical methods. In the second part of the contribution, we study the longitudinal asymmetry $A_z^{n\,{}^3\mathrm{He}}$ in the ${}^3\mathrm{He}(\mathbf{n}, p){}^3\mathrm{H}$ reaction in order to obtain information about the parity-violating components of the nucleon–nucleon interaction.

## 1 Introduction

In recent years, there has been a rapid advance in the ability to obtain accurate solutions of the four-nucleon (4N) scattering problem with realistic Hamiltonians. Accurate calculations of four-body scattering observables have been achieved in the framework of the Alt–Grassberger–Sandhas (AGS) equations [1], solved in momentum space, where the long-range Coulomb interaction is treated using the screening and renormalization method [2,3]. Also quite well converged solutions of either the Faddeev–Yakubovsky (FY) equations in configuration space [4,5] or the Hyperspherical Harmonics (HH) expansion method [6] have been reported [7,8].

The effort for solving the 4N scattering problem is motivated by the necessity to investigate the ability of the different models of the nucleon-nucleon (NN) and three-nucleon (3N) interactions to reproduce the experimental data in systems with $A > 3$. Clearly, first of all, it is necessary to establish the accuracy reached by the theoretical methods in the solution of this problem. In a previous benchmark, the results obtained by different groups working with different techniques were found to be at variance with each other [9]. In the first part of the present paper, we compare the new results obtained by means of the HH expansion method to the calculations performed by solving the AGS and FY equations (a more extended comparison can be found in Ref. [10]).

M. Viviani (✉) · A. Kievsky · L. E. Marcucci
INFN, Sezione di Pisa, 56127 Pisa, Italy
E-mail: michele.viviani@pi.infn.it

L. Girlanda
Physics Department, Università del Salento, 73100 Lecce, Italy

L. Girlanda
INFN, Sezione di Lecce, 73100 Lecce, Italy

L. E. Marcucci
Physics Department, Università di Pisa, 56127 Pisa, Italy

The potentials used in this paper are the I-N3LO model by Entem and Machleidt [11], with cutoff $\Lambda = 500$ MeV, the Argonne $v_{18}$ (AV18) potential model [12], and a low-$k$ model derived from the CD-Bonn potential [13]. The I-N3LO potential has been derived using an effective field theory approach and the chiral perturbation theory up to next-to-next-to-next-to-leading order. The AV18 potential is a phenomenological potential having a rather strong repulsion at short interparticle distances. The low-$k$ potentials have been obtained separating the Hilbert space into low and high momentum regions and using the renormalization group method [13] to integrate out the high-momentum components above a cutoff $\Lambda$. The low-$k$ potential adopted in this work is obtained starting from the realistic CD-Bonn potential [14] and using a smooth cutoff $\Lambda = 2.5$ fm$^{-1}$. The cut of the high-momentum part is reflected in configuration space in an almost total absence of the repulsion at short interparticle distances. Note that the first and third model are non-local, while AV18 is local in configuration space. The three potentials reproduce equally well the $np$ and $pp$ data, and are a representative set of the large variety of modern NN potential models. We note finally that I-N3LO and AV18 interactions, without the inclusion of a suitable 3N interaction model, largely underestimate the $^4$He binding energy $B(^4\text{He})$. On the contrary, with the adopted low-$k$ potential model we have $B(^4\text{He}) = 29.04$ MeV, slightly overestimating the experimental value of 28.30 MeV.

In the second part of the present paper, we discuss the study of a parity-violating (PV) observable in the reaction $\mathbf{n} + {}^3\text{He} \to p + {}^3\text{H}$. The primary objective of this study is to determine the fundamental parameters of hadronic weak interactions [15], in particular the strength of the long-range part of the PV NN potential, mediated by one-pion exchange (OPE).

This paper is organized as follows. In Sect. 2, a brief description of our technique (the HH expansion) used to solve the 4N scattering problem is reported. In Sect. 3, the results of the benchmark performed with the AGS and FY techniques are shown. In Sect. 4, we present the study of the reaction $\mathbf{n} + {}^3\text{He} \to p + {}^3\text{H}$. The conclusions will be given in Sect. 5.

## 2 The HH Method

In this section, a brief description of our technique (the HH expansion) used to solve the 4N scattering problem is reported. The total kinetic energy, $T_{c.m.}$, in the center of mass (c.m.) and the nucleon kinetic energy, $E_N$ ($N = p, n$), in the laboratory reference frame, are given by

$$T_{c.m.} = \frac{q^2}{2\mu}, \quad E_N = \frac{4}{3} T_{c.m.}, \tag{1}$$

where $\mu = (3/4) M_N$ is the reduced mass of the $1 + 3$ system, $M_N$ is the nucleon mass, and $q$ the magnitude of the relative momentum between the two clusters.

The wave function describing a $n - {}^3\text{H}$ or $p - {}^3\text{He}$ scattering state with total angular momentum quantum numbers $J$, $J_z$, incoming relative orbital angular momentum $L$, and channel spin $S$ ($S = 0, 1$) can be written as

$$\Psi_{1+3}^{LS,JJ_z} = \Psi_C^{LS,JJ_z} + \Psi_A^{LS,JJ_z}, \tag{2}$$

where the part $\Psi_C^{LS,JJ_z}$ describes the system in the region where the particles are close to each other and their mutual interactions are strong. Hence, $\Psi_C^{LS,JJ_z}$ vanishes in the limit of large inter-cluster distances. This part of the wave function is written as a linear expansion $\sum_\mu c_\mu^{LSJ} \mathcal{Y}_\mu$, where $\mathcal{Y}_\mu$ is a set of basis functions constructed in terms of the HH functions (for more details, see, for example, Ref. [6]).

The other part $\Psi_A^{LS,JJ_z}$ describes the relative motion of the two clusters in the asymptotic region, where the $1 + 3$ interaction is negligible (except eventually for the long-range Coulomb interaction).

In the asymptotic region the wave functions $\Psi_{1+3}^{LS,JJ_z}$ reduces to $\Psi_A^{LS,JJ_z}$, which must therefore be the appropriate asymptotic solution of the Schrödinger equation. Let us consider, for example, the $p - {}^3\text{He}$ case. Then, $\Psi_A^{LS,JJ_z}$ can be decomposed as a linear combination of the following functions

$$\Omega_{LS,JJ_z}^{\pm} = \sum_{l=1}^{4} [Y_L(\hat{\boldsymbol{y}}_l) \otimes [\phi_3(ijk) \otimes s_l]_S]_{JJ_z} \left( f_L(y_l) \frac{G_L(\eta, q y_l)}{q y_l} \pm \mathrm{i} \frac{F_L(\eta, q y_l)}{q y_l} \right), \tag{3}$$

where $\boldsymbol{y}_l$ is the distance between the proton (particle $l$) and $^3$He (particles $ijk$), $q$ is the magnitude of the relative momentum between the two clusters, $s_l$ the spin state of particle $l$, and $\phi_3$ is the $^3$He wave function. Moreover,

$F_L$ and $G_L$ are the regular and irregular Coulomb function, respectively, with $\eta = 2\mu e^2/q$. The function $f_L(y) = [1 - \exp(-\beta y)]^{2L+1}$ in Eq. (3) has been introduced to regularize $G_L$ at small $y$, and $f_L(y) \to 1$ as $y$ is large, thus not affecting the asymptotic behavior of $\Psi_{1+3}^{LS,JJ_z}$. Note that for large values of $qy_l$,

$$f_L(y_l)G_L(\eta, qy_l) \pm \mathrm{i}F_L(\eta, qy_l) \to \exp[\pm\mathrm{i}(qy_l - L\pi/2 - \eta\ln(2qy_l) + \sigma_L)], \tag{4}$$

where $\sigma_L$ is the Coulomb phase-shift. Therefore, $\Omega^+_{LS,JJ_z}$ ($\Omega^-_{LS,JJ_z}$) describe the asymptotic outgoing (ingoing) $p - {}^3$He relative motion. If necessary, the long-range magnetic moment interaction can also be taken into account [16]. Finally,

$$\Psi_A^{LS,JJ_z} = \sum_{L'S'}[\delta_{LL'}\delta_{SS'}\Omega^-_{LS,JJ_z} - \mathcal{S}^{J\pi}_{LS,L'S'}\Omega^+_{L'S',JJ_z}], \tag{5}$$

where the parameters $\mathcal{S}^{J\pi}_{LS,L'S'}$ are the $S$-matrix elements which determine phase-shifts and (for coupled channels) mixing parameters at the energy $T_{c.m.}$. Of course, the sum over $L'$ and $S'$ is over all values compatible with the given $J$ and parity $\pi$. In particular, the sum over $L'$ is limited to include either even or odd values such that $(-1)^{L'} = (-)^L = \pi$.

The $S$-matrix elements $\mathcal{S}^{J\pi}_{LS,L'S'}$ and coefficients $c_\mu^{LSJ}$ occurring in the HH expansion of $\Psi_C^{LS,JJ_z}$ are determined by making the functional

$$\left[\mathcal{S}^{J\pi}_{LS,L'S'}\right] = \mathcal{S}^{J\pi}_{LS,L'S'} - \left\langle \Psi_{1+3}^{L'S',JJ_z}|H - E|\Psi_{1+3}^{LS,JJ_z}\right\rangle \tag{6}$$

stationary with respect to variations in the $\mathcal{S}^{J\pi}_{LS,L'S'}$ and $c_\mu^{LSJ}$ (Kohn variational principle). In the above equation, $E = T_{c.m.} - B({}^3\mathrm{He})$ is the energy of the system, $B({}^3\mathrm{He})$ being the ${}^3$He binding energy. By applying this principle, a linear set of equations is obtained for $\mathcal{S}^{J\pi}_{LS,L'S'}$ and $c_\mu^{LSJ}$. This linear system is solved using the Lanczos algorithm.

This method can be applied in either coordinate or momentum space, and using either local or non-local potentials [6] (see also Ref. [17] for an application to the $A = 3$ system). The first step is a partial wave decomposition of the asymptotic functions $\Omega^\pm_{LS,JJ_z}$, a task which can be rather time consuming, in particular for the $J^\pi = 2^-$ state. After this decomposition, the calculation of the matrix element in Eq. (6) is fast. Then, the problem reduces to the solution of the linear system, which is performed using an iterative method (however, this solution has to be repeated several times due to the necessity to extrapolate the results, see below).

The expansion of the scattering wave function in terms of the HH basis is in principle infinite, therefore a truncation scheme is necessary. The HH functions are essentially characterized by the orbital angular momentum quantum numbers $\ell_i$, $i = 1, 2, 3$, associated with the three Jacobi vectors, and the grand angular quantum number $K$ (each HH function is a polynomial of degree $K$). The basis is truncated to include states with $\ell_1 + \ell_2 + \ell_3 \le \ell_{\max}$ (with all possible re-coupling between angular and spin states appropriate to the given $J$). Between these states, we retain only the HH functions with $K \le K_{\max}$. In the calculation we have included only states with total isospin $T = 1$.

The numerical uncertainty comes from the numerical integrations needed to compute the matrix elements of the Hamiltonian and the truncation of the basis. It has been checked that the numerical uncertainty of the calculated phase-shifts related to the numerical integration is small (around 0.1 %). The NN interaction has been limited to act on two-body states with total angular momentum $j \le j_{\max} = 8$ (at the considered energies, greater values of $j_{\max}$ are completely unnecessary). The largest uncertainty is thus related to the use of a finite basis. The convergence with $\ell_{\max}$ is rather fast and the value $\ell_{\max} = 6$ have been found to be sufficient. The main problem is related to the slow convergence of the results with $K_{\max}$. This problem can be partly overcome by performing calculations for increasing values of $K_{\max}$ and then using some extrapolation rule (see for example Ref. [18]) to get the "$K_{\max} \to \infty$" result. This procedure has an uncertainty which can be estimated. A detailed study of this problem will be published elsewhere [19]. The convergence of the quantities of interest in term of $K_{\max}$ is slower when NN potentials with a strong repulsion at short interparticle distance are used such as for the AV18 potential. In this case we have estimated the uncertainty to be of the order of 0.5 % in the extrapolated phase-shifts. This problem is less relevant for the I-N3LO and the low-$k$ models. In these cases, the uncertainty has been estimated to be at most 0.3 %.

## 3 Results of the Benchmark

In this section, we show the results of the benchmark performed between the HH, AGS and FY techniques. We have considered the differential cross section and the neutron (proton) analyzing power $A_{y0}$ for $n - {}^3\mathrm{H}$ ($p - {}^3\mathrm{He}$) elastic scattering at the considered energies, as functions of the c.m. scattering angle. Furthermore, we have also considered the triton (${}^3\mathrm{He}$) analyzing power $A_{0y}$. This observable is in fact rather sensitive to small variations of the phase-shifts in the kinematical regime considered in this paper.

In Figs. 1 and 2 we have reported the results obtained using the AGS equation (solid lines), the HH expansion method (dashed lines), and the FY equations (dotted lines) using the I-N3LO potential. As can be seen by

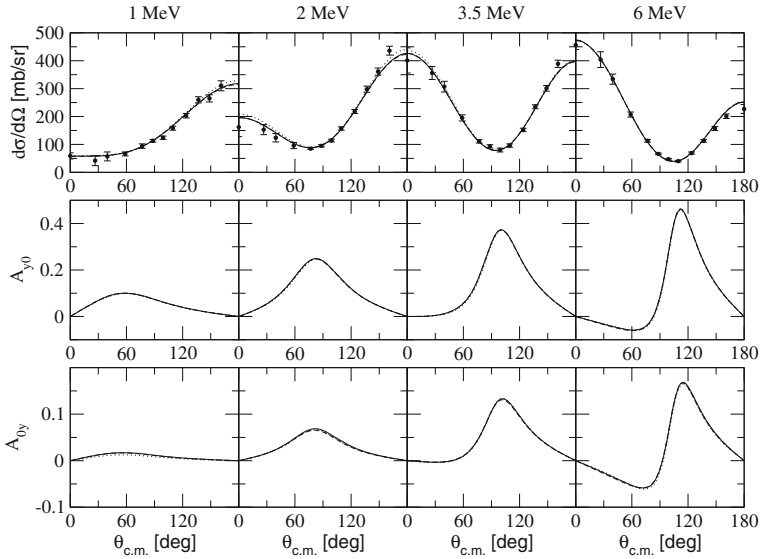


**Fig. 1** Differential cross section and neutron and triton analyzing powers $A_{y0}$ and $A_{0y}$ for $n - {}^3\mathrm{H}$ elastic scattering at $E_n = 1$, 2, 3.5, and 6 MeV neutron lab energies as functions of the c.m. scattering angle. Results obtained using the AGS equation (*solid lines*), the HH expansion method (*dashed lines*), and the FY equations (*dotted lines*) using the I-N3LO potential are compared. For most of the cases the three curves coincide and cannot be distinguished. The experimental data are from Ref. [20]

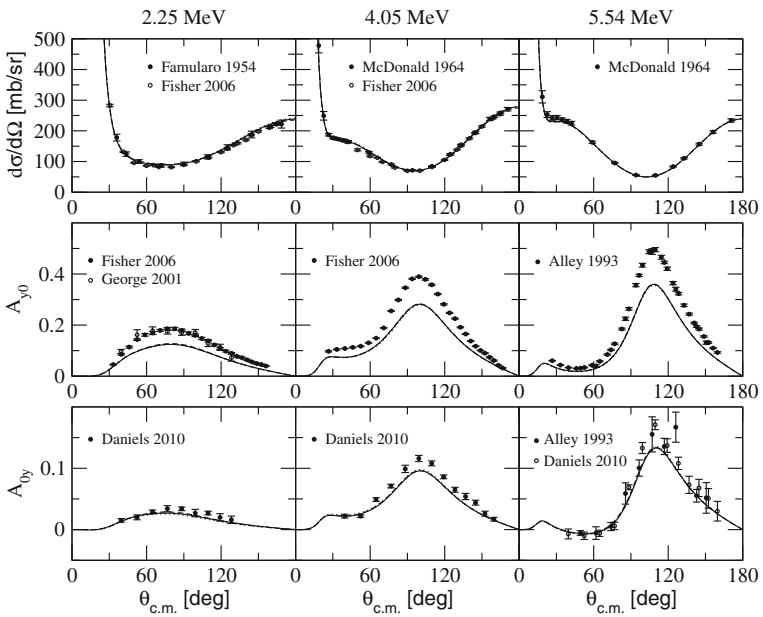


**Fig. 2** Same as Fig. 1, but for $p - {}^3\mathrm{He}$ elastic scattering at $E_p = 2.25$, 4.05, and 5.54 MeV proton lab energies. The experimental data are from Refs. [18,21–25]

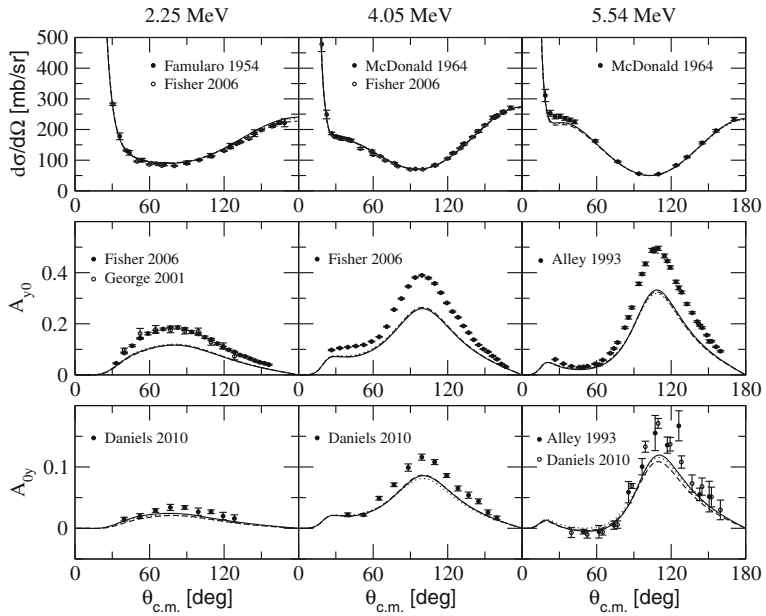


**Fig. 3** Same as Fig. 2, but for the AV18 potential

inspecting the two figures, the three curves almost always perfectly coincide and cannot be distinguished. We have also reported the experimental data for the $n - {}^3$H differential cross section [20] and the three $p - {}^3$He observables [18,21–25]. We note that the differences between the three calculations, where they can be appreciated, are in any case always smaller than the experimental errors.

For the other two potentials, we show the comparison only for $p - {}^3$He scattering. The agreement between the three calculations when the AV18 potential is adopted is again rather satisfactory, as can be seen in Fig. 3. A small disagreement can be observed only for the $A_{0y}$ observable (see the panels in the last row of Fig. 3). This observable is also rather sensitive to the small $D$-wave and $F$-wave phase-shifts. We already know that the AV18 model contains a stronger repulsion at short interparticle distance than the I-N3LO. As discussed above, the convergence of the HH method for this case is more problematic and consequently the calculations have a larger uncertainty. In spite of these difficulties, the agreement in the considered observables is still quite good.

Let us consider now the low-$k$ potential, which has no repulsion at short interparticle distance. Consequently, in this case, we expect a good agreement between the results of the different techniques. For this potential, the calculations have been performed using the AGS (solid curves) and HH (dashed curves) methods, only. From Fig. 4, we see that, as expected, the results are practically indistinguishable, confirming that for soft potentials the convergence of the calculations is excellent.

Finally, in the literature for $p - {}^3$He scattering, there exist measurements of other spin correlation observables ($A_{yy}$, $A_{xx}$, $A_{zz}$, $A_{xz}$, and $A_{zx}$). Also for these observables we have found a good agreement between the predictions obtained by the three different methods, for all the potential models considered here.

## 4 The $^3$He(n, $p$)$^3$H Longitudinal Asymmetry

For ultracold neutrons, the longitudinal asymmetry $A_z^{n^3\mathrm{He}}$ for the reaction $^3$He(**n**, $p$)$^3$H is given by $A_z^{n^3\mathrm{He}} = a_z \cos\theta$ [26], where $\theta$ is the angle between the outgoing proton momentum and the neutron beam direction. The coefficient $a_z$ can be expressed in terms of products of $T$-matrix elements involving three parity-conserving (PC) and three PV transitions (see Ref. [26] for more details). The PV $T$-matrix elements are calculated as mean values of the PV interaction between 4N scattering states. The latter quantities have been obtained as discussed in Sect. 2 by means of the HH method and using the I-N3LO NN potential plus the N-N2LO 3N interaction model [27].

Until recently, the standard setting by which nuclear PV processes were analyzed theoretically was the use of potentials derived from the usual meson-exchange mechanism, in particular using the model proposed by

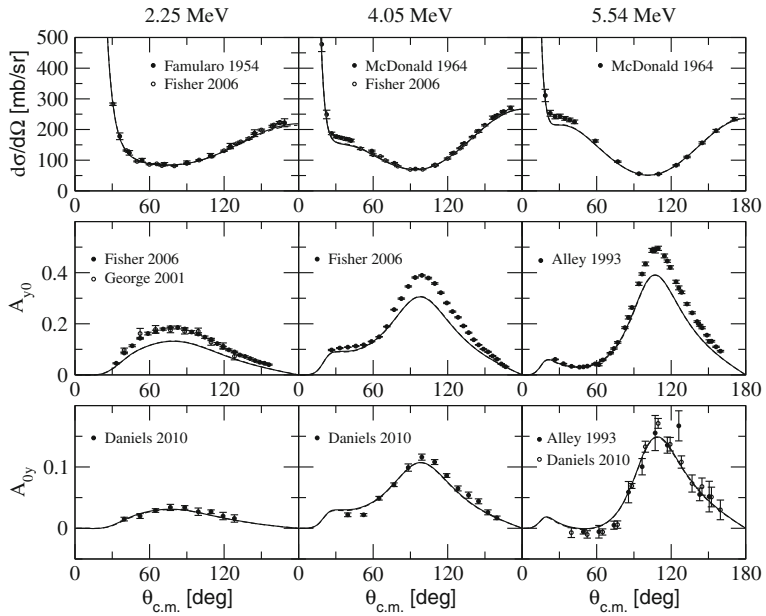


**Fig. 4** Same as Fig. 2, but for the low-$k$ potential. Only the AGS and HH results are reported

Desplanques, Donoghue, and Holstein (DDH) [28]. In recent years, a new, more systematic, approach based in a model-independent field-theoretic treatment of the nuclear forces has been vigorously pursued [29–31]. In this effective field theory (EFT) approach the pion couples to nucleons by powers of its momentum $Q$, and the Lagrangian describing these interactions can be expanded in powers of $Q/\Lambda_\chi$, where $\Lambda_\chi \sim 1$ GeV specifies the chiral-symmetry breaking scale. The EFT has been used to describe also the PV components in the NN interaction. Kaplan and Savage [32] wrote in a pioneering work an effective Lagrangian describing the PV interaction of pions and nucleons up to one derivative. This Lagrangian includes a "Yukawa" pion–nucleon interaction with no derivatives, multiplied by a parameter denoted as $h_\pi^1$ and known as the "weak pion–nucleon" coupling constant. It gives the long-range OPE contribution to the PV NN interaction.

The PV NN potential at next-to-next-to-leading (N2LO) was derived for the first time by Zhu et al. [33]. This potential includes the long-range OPE component, medium-range components originating from two-pion exchange (TPE) processes, and short-range components deriving from *ten* four-nucleon contact terms (the Authors of Ref. [33] noted that at low energy their ten contact interactions collapse into *five* independent operators, corresponding to the five S–P low-energy PV amplitudes [34]). In a series of other works, Desplanques et al. have also derived the contribution of the TPE diagrams at N2LO [35] to study, in particular, PV effects in the capture reaction $^1$H(**n**, $\gamma$)$^2$H. The expression of the TPE contribution obtained by Desplanques et al. is slightly different from that one reported by Zhu et al. [33].

We have recently derived again the PV NN potential at N2LO, in order to clarify the exact expression of the TPE contribution. Moreover, the more recent analysis of Ref. [36] has shown that actually there exist only *five* independent contact terms with one derivative. We give a short summary of the properties of this PV potential below. It contains six unknown parameters, the pion-nucleon PV coupling constant $h_\pi^1$ and five low-energy constants (LEC's).

### 4.1 The PV Interaction

The potential can be constructed using time-ordered perturbation theory, following the same approach as for the PC potential described in Ref. [37]. The different diagrams contributing to the PV NN potential up to order $\mathcal{O}(Q)$ are shown in Fig. 5. The OPE diagram (a) gives the lowest order (LO) contribution (of order $Q^{-1}$). There is no contribution of order $Q^0$, but there are several contributions of order $Q^1$ (namely, at N2LO): a relativistic correction coming from diagram (a), TPE contributions coming from diagrams (d), (f), and (g), and five contact interactions described by diagram (CT). The contributions of diagrams (b) and (c) vanish due to the integration over the loop variable, while those of diagrams (e) and (h) (vertex corrections) can be

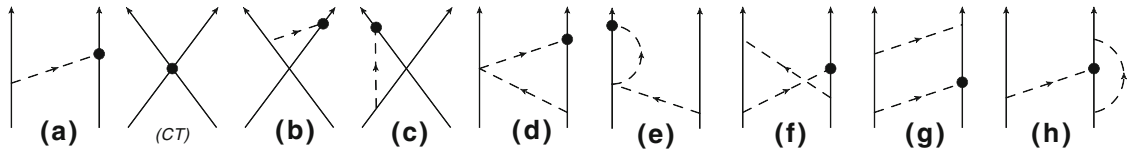


**Fig. 5** Time-ordered diagrams contributing to the PV potential (only one time ordering is given). Nucleons and pions are denoted by *solid* and *dashed lines*. The *solid dot* represents a PV vertex

reabsorbed by a redefinition of the coupling constant $h_\pi^1$. More details on the derivation of the potential will be reported elsewhere [38].

In order to transform this potential in $r$-space, we have to multiply the expressions reported above by a cutoff, which has been chosen as

$$f_\Lambda(k) = \exp(-(k/\Lambda)^4), \tag{7}$$

where $\Lambda = 500 \div 700$ MeV is a cutoff parameter. With such a choice (a function which depends on $k$ only), the resulting potential is local. The potential contains six unknown parameters, the pion–nucleon PV coupling constant $h_\pi^1$ and five LEC's $C_i$, $i = 1, \ldots, 5$ multiplying the contact interactions. In addition, the potential will depend on the cutoff parameter $\Lambda$ needed to cut the potential at high $k$. A first estimate for these LEC's can be obtained by comparing the chiral potential with the DDH model [28]. We have found $C_2 \approx 10^{-6}$, while the other LEC's are moreless of the order of $10^{-7}$ [19].

Some of the LEC's can be fixed using the following three accurate measurements of the angle-averaged $\mathbf{p}$–$p$ longitudinal asymmetry $\overline{A}_z^{pp}(E)$, obtained at different laboratory energies $E$:

$$\begin{aligned}
&\overline{A}_z^{pp}(13.6\text{ MeV}) = (-0.97 \pm 0.20) \times 10^{-7}, [39],\\
&\overline{A}_z^{pp}(45\text{ MeV}) = (-1.53 \pm 0.21) \times 10^{-7}, [40],\\
&\overline{A}_z^{pp}(221\text{ MeV}) = (+0.84 \pm 0.34) \times 10^{-7}, [41].
\end{aligned} \tag{8}$$

Using the PV potential derived from EFT, and taking into account the matrix elements of the different isospin operators, the longitudinal asymmetry at the end can be expressed as

$$\overline{A}_z^{pp}(E) = a_0(E)h_\pi^1 + a_1(E)C_1' + a_2(E)C_2, \tag{9}$$

where $C_1' = C_1 + 2C_4 + 2C_5$ and $a_0(E)$, $a_1(E)$ e $a_2(E)$ are numerical coefficients independent from the values of the LEC's (however, they depend on $\Lambda$). We would like to fix the three unknown parameters $h_\pi^1$, $C_1'$, and $C_2$ imposing that at the three given energies the longitudinal asymmetry of Eq. (9) reproduces the experimental values of Eq. (8). However, the values of $a_i$ at low energy scale as $\sqrt{E}$, since the longitudinal asymmetry is dominated by the contribution of $S$-waves. In practice, the experimental data at $E = 13.6$ MeV and $E = 45$ MeV are equivalent and the number of independent equations reduces to two.

It is therefore necessary to fix the value of one of the constant to determine the remaining two. In the following, we assume that the $h_\pi^1$ value be in the "reasonable range" discussed in Ref. [28]. In particular we perform the calculations for three values of the coupling constant $h_\pi^1$:

1. $h_\pi^1 = 4.56 \times 10^{-7}$ ("best choice")
2. $h_\pi^1 = 0$ (minimum value of the "reasonable range")
3. $h_\pi^1 = 11.4 \times 10^{-7}$ (maximum value of the "reasonable range")

The values of $C_1'$ and $C_2$, corresponding to the three choices of $h_\pi^1$ and determined in order to reproduce the experimental longitudinal asymmetries at 45 and 221 MeV, are reported in Table 1.

### 4.2 Results

In Table 2, we present the results of a *preliminary* calculation of $a_z$ for the various choices of $h_\pi^1$ and $\Lambda$, by taking the values of $C_1'$ and $C_2$ from Table 1, and assuming $C_1 = C_1'$ and $C_{3,4,5} = 0$. We observe that $A_z^{n^3\text{He}}$ is dominated by the contribution of the (isovector) LO OPE potential. Naively, one expects that the

**Table 1** Coefficients $C_1'$ and $C_2$ for different values of $h_\pi^1$ and $\Lambda$ determined to reproduce the experimental values of $\overline{A}_z^{pp}$ at 45 and 221 MeV

| $\Lambda$ (MeV) | $C_1'$ | $C_2$ | $C_1'$ | $C_2$ | $C_1'$ | $C_2$ |
|---|---|---|---|---|---|---|
| | $h_\pi^1 = 4.56 \times 10^{-7}$ | | $h_\pi^1 = 0$ | | $h_\pi^1 = 11.4 \times 10^{-7}$ | |
| 500 | −2.15516 | 9.98171 | −1.51765 | 4.00256 | −3.11142 | 18.9504 |
| 600 | −2.69957 | 10.03513 | −2.18203 | 4.42237 | −3.47588 | 18.4543 |
| 700 | −4.22214 | 10.66532 | −4.68110 | 5.86730 | −3.53372 | 17.8623 |

**Table 2** The coefficient $a_z$ (in units of $10^{-7}$) describing the $^3$He(**n**, $p$)$^3$H longitudinal asymmetry (*preliminary* results).

| | $h_\pi^1 = 4.56 \times 10^{-7}$ | | $h_\pi^1 = 0$ | | $h_\pi^1 = 11.4 \times 10^{-7}$ | |
|---|---|---|---|---|---|---|
| | OPE/LO | FULL | OPE/LO | FULL | OPE/LO | FULL |
| 500 | −0.551 | −0.544 | 0.000 | +0.044 | −1.377 | −1.425 |
| 600 | −0.554 | −0.578 | 0.000 | +0.034 | −1.385 | −1.497 |
| 700 | −0.546 | −0.584 | 0.000 | +0.009 | −1.366 | −1.473 |

The calculations are performed using the I-N3LO NN plus the N-N2LO 3N potentials for the PC interaction, and the chiral PV potential model discussed in this paper for various choices of the pion–nucleon coupling constant $h_\pi^1$ and the cutoff parameter $\Lambda$. The corresponding values of the LEC's $C_i$, $i = 1, \ldots, 5$ are discussed in the text. In the columns labeled "OPE/LO" we have reported the values of $a_z$ calculated by retaining in the PV potential only the LO OPE contribution, while in the columns labeled "FULL" we have included all terms

most important contribution would come from the isoscalar operators (those multiplied by the LEC's $C_1$ and $C_2$). In fact, at this energy, the reaction proceeds mainly through the close $0^+$ and $0^-$ resonances, which are considered to have total isospin $T = 0$ [42]. Thus, the isoscalar operators in the PV potential should give the dominant contribution. However, the Coulomb interaction in the final state induces sizable isospin mixing configurations and, since the LO OPE term is the longest range term, at the end it gives the most important contribution, except the case where $h_\pi^1$ is close to zero. The contribution of the relativistic correction to the LO OPE is always very tiny. For the case $h_\pi^1 = 0$, $a_z$ is given mainly by the contribution of the isoscalar operator multiplying the LEC $C_2$.

Let us discuss now the dependence of $a_z$ on the LEC's $C_{3,4,5}$. Due to some cancellations between the contributions coming from the TPE and the different contact interaction terms, we have found a noticeable sensitivity to these LEC's, of the order of 20%. Therefore, the measure of this observable could be very useful to extract them. From the table, we observe also that $a_z$ does not depend very much on $\Lambda$. This dependence in some measure gives indication of the importance of high order contributions. The fact that it is found to be weak, it gives confidence that the PV potential at N2LO represents a good description of the NN PV potential.

## 5 conclusion

In the first part of this work, we have shown that for I-N3LO and the selected low-$k$ potential model, which have a "soft" repulsion at short interparticle distances (the low-$k$ model has no repulsion at all), the results obtained by the different techniques used to solve the 4N scattering problem are in very good agreement. With the AV18 potential, the agreement is not so perfect, although the (slight) differences can be appreciated only for some small polarization observables. We can conclude therefore that the $A = 4$ scattering problem is nowadays solved with a very good accuracy, better than 1%.

Concerning the comparison with the experimental data, we have confirmed the large under prediction of the $p - {}^3$He $A_{y0}$ observable, a problem already put in evidence some time ago [4,24,43], and certainly related to the $N - d$ "$A_y$ puzzle". For this observable we have observed a moderate dependence on the considered potential models. The discrepancies found, in particular for $A_{y0}$, indicate a serious difficulty of the existing NN force models in describing the 4N continuum. This difficulty can hardly be solved by the inclusion of a standard type 3NF, used to reproduce the few-nucleon binding energies [8,9,18]. Its origin could rather lie either in the NN forces themselves, or in the presence of a 3NF of unknown type. Clearly, an eventual solution of the $A = 4$ $A_{y0}$ problem should be related in some way to the solution of the $N - d$ "$A_y$ puzzle". Recently, new models of 3N forces have been proposed [44,45], their effects on the 3N and 4N continuum is under study.

In this contribution, we have also presented a *preliminary* study of the longitudinal asymmetry in $^3$He(**n**, $p$)$^3$H using a PV NN potential derived from an effective field theory framework at next-to-next-to-

leading order, including one- and two-pion exchanges, contact interactions and relativistic corrections. This potential depends on six low-energy constants. Some of these parameters have been constrained to reproduce the existing accurate measurements of the **p**-$p$ longitudinal asymmetry. Using these constraints we compute $A_z^{n^3\mathrm{He}}$ and study the sensitivity of such an observable to the unconstrained parameters. The main motivation of this study is related to the goal of understanding the hadronic weak interaction, in particular its long-range contribution related to the OPE. To be noticed that a number of experiments aimed at studying parity violation in low-energy processes involving few nucleon systems are being completed or are in an advanced stage of planning at cold neutron facilities, such as the Los Alamos Neutron Science Center, the NIST Center for Neutron Research, and the Spallation Neutron Source at Oak Ridge.

## References


1. Deltuva, A., Fonseca, A.C.: Four-nucleon scattering: ab initio calculations in momentum space. Phys. Rev. C **75**, 014005 (2007)
2. Alt, E.O., Sandhas, W., Ziegelmann, H.: Coulomb effects in three-body reactions with two charged particles. Phys. Rev. C **17**, 1981 (1978)
3. Deltuva, A., Fonseca, A.C., Sauer, P.U.: Momentum-space description of three-nucleon breakup reactions including the Coulomb interaction. Phys. Rev. C **72**, 054004 (2005)
4. Ciesielski, F., Carbonell, J.: Solutions of the Faddeev–Yakubovsky equations for the four nucleon scattering states. Phys. Rev. C **58**, 58 (1998)
5. Lazauskas, R.: Elastic proton scattering on tritium below the n-3He threshold. Phys. Rev. C **79**, 054007 (2009)
6. Kievsky, A. et al.: A high-precision variational approach to three- and four-nucleon bound and zero-energy scattering states. J. Phys. G Nucl. Part. Phys. **35**, 063101 (2008)
7. Viviani, M. et al.: Neutron–triton elastic scattering. Few Body Syst. **45**, 119 (2009)
8. Viviani, M. et al.: Proton-$^3$He elastic scattering at low energies and the Ay Puzzle. EPJ Web Conf. **3**, 05011 (2010)
9. Lazauskas, R. et al.: Low energy $n-{}^3$H scattering: a novel testground for nuclear interactions. Phys. Rev. C **71**, 034004 (2005)
10. Viviani, M. et al.: Benchmark calculation of $n-{}^3$H and $p-{}^3$He scattering. Phys. Rev. C **84**, 054010 (2011)
11. Entem, D.R., Machleidt, R.: Accurate charge-dependent nucleon–nucleon potential at fourth order of chiral perturbation theory. Phys. Rev. C **68**, 041001 (2003)
12. Wiringa, R.B., Stoks, V.G.J., Schiavilla, R.: Accurate nucleon–nucleon potential with charge-independence breaking. Phys. Rev. C **51**, 38 (1995)
13. Bogner, S.K., Kuo, T.T.S., Schwenk, A.: Model-independent low momentum nucleon interaction from phase shift equivalence. Phys. Rep. **386**, 1 (2003)
14. Machleidt, R.: High-precision, charge-dependent Bonn nucleon–nucleon potential. Phys. Rev. C **63**, 024001 (2001)
15. Ramsey-Musolf, M.J., Page, S.A.: Hadronic parity violation: a new view through the looking glass. Ann. Rev. Nucl. Part. Sci. **56**, 1 (2006)
16. Kievsky, A., Viviani, M., Marcucci, L.E.: $N-d$ scattering including electromagnetic forces. Phys. Rev. C **69**, 014002 (2004)
17. Marcucci, L.E. et al.: $N-d$ elastic scattering using the hyperspherical harmonics approach with realistic local and nonlocal interactions. Phys. Rev. C **80**, 034003 (2009)
18. Fisher, B.M. et al.: Proton-$^3$He elastic scattering at low energies. Phys. Rev. C **74**, 034001 (2006)
19. Viviani, M., et al.: (in preparation)
20. Seagrave, J.D., Cranberg, L., Simmons, J.E.: Elastic scattering of fast neutrons by tritium and $^3$He. Phys. Rev. **119**, 1981 (1960)
21. Famularo, K.F., et al.: Differential cross sections for elastic scattering of protons by $^3$He. Phys. Rev. **93**, 928
22. McDonald, D.G., Haberli, W., Morrow, L.W.: Polarization and cross section of protons scattered by $^3$He from 4 to 13 MeV. Phys. Rev. **133**, B1178 (1964)
23. Alley, M.T., Knutson, L.D.: Spin correlation measurements for $p-{}^3$He elastic scattering between 4.0 and 10.0 MeV. Phys. Rev. C **48**, 1890 (1993)
24. Viviani, M. et al.: The $A_y$ problem for $p-{}^3$He elastic scattering. Phys. Rev. Lett. **86**, 3739 (2001)
25. Daniels, T.V. et al.: Spin-correlation coefficients and phase-shift analysis for $p+{}^3$He elastic scattering. Phys. Rev. C **82**, 034002 (2010)
26. Viviani, M., Schiavilla, R., Girlanda, L., Kievsky, A., Marcucci, L.E.: Parity-violating asymmetry in the $^3$He(**n**, )$p^3$H reaction. Phys. Rev. C **82**, 044001 (2010)
27. Navrátil, P.: Local three-nucleon interaction from chiral effective field theory. Few Body Syst. **41**, 117 (2007)
28. Desplanques, B., Donoghue, J.F., Holstein, B.R.: Unified treatment of the parity violating nuclear force. Ann. Phys. (N.Y.) **124**, 449 (1980)
29. Weinberg, S.: Nuclear forces from chiral lagrangians. Phys. Lett. B **251**, 288 (1990)
30. Epelbaum, E., Hammer, H.W., Meissner, U.G.: Modern theory of nuclear forces. Rev. Mod. Phys. **81**, 1773 (2009)
31. Machleidt, R., Entem, D.R.: Chiral effective field theory and nuclear forces. Phys. Rep. **503**, 1 (2011)
32. Kaplan, D.B., Savage, M.J.: An analysis of parity-violating pion–nucleon couplings. Nucl. Phys. A **556**, 653 (1993)
33. Zhu, S.L., Maekawa, C.M., Holstein, B.R., Ramsey-Musolf, M.J., Kolck, U.van : Nuclear parity violation in effective field theory. Nucl. Phys. A **748**, 435 (2005)

34. Danilov, G.S.: Circular polarization of $\gamma$ quanta in absorption of neutrons by protons and isotopic structure of weak interactions. Phys. Lett. **18**, 40 (1965)
35. Desplanques, B., Hyun, C.H., Ando, S., Liu, C.P.: Parity-violating nucleon–nucleon interaction from different approaches. Phys. Rev. C **77**, 64002 (2008)
36. Girlanda, L.: Redundancy in the parity-violating 2-nucleon contact Lagrangian. Phys. Rev. C **77**, 067001 (2008)
37. Pastore, S., Girlanda, L., Schiavilla, R., Viviani, M., Wiringa, R.B.: Electromagnetic currents and magnetic moments in chiral effective field theory ($\chi$EFT). Phys. Rev. C **80**, 034004 (2009)
38. Viviani, M., Baroni, A., Girlanda, L., Kievsky, A., Marcucci, L.E., Schiavilla, R. (in preparation)
39. Eversheim, P.D. et al.: Phys. Lett. **B256**, 11 (1991)
40. Kistryn, S. et al.: Precision measurement of parity nonconservation in proton-proton scattering at 45 MeV. Phys. Rev. Lett. **58**, 1616 (1987)
41. Berdoz, A.R. et al.: Parity violation in proton–proton scattering at 221 MeV. Phys. Rev. C **68**, 034004 (2003)
42. Tilley, D.R., Weller, H.R., Hale, G.M.: Energy levels of light nuclei $A = 4$. Nucl. Phys. A **541**, 1 (1992)
43. Fonseca, A.C.: Contribution of nucleon–nucleon P waves to nt-nt, dd-pt, and dd-dd scattering observables. Phys. Rev. Lett. **83**, 4021 (1999)
44. Bernard, V., Epelbaum, E., Krebs, H., Meissner, Ulf-G.: Subleading contributions to the chiral three-nucleon force. II. Short-range terms and relativistic corrections. Phys. Rev. C **84**, 054001 (2011)
45. Girlanda, L., Kievsky, A., Viviani, M.: Subleading contributions to the three-nucleon contact interaction. Phys. Rev. C **84**, 014001 (2011)